SUPPLEMENTARY METHODS

Human Cell Lines

RMS559 were obtained from J. Fletcher, Brigham and Women's Hospital. RH30 (J. Khan) and K562 (C. Guidos) were also used in this study. Cell line identities were verified with STR Analysis. Cells were tested for mycoplasma.

PCR Analysis

Proviral integration and transgene representation was examined in genomic DNA isolated from myoblasts and tumor tissue with DNeasy (Qiagen) and utilizing PCR primers and conditions detailed in Supplemental Table 1. Real-time PCR quantified expression levels of specific genes in cells and tissues as described in Supplemental Methods.

Protein expression analysis

Myoblasts were seeded and plated in MGM overnight. The following day, cells were washed twice with PBS, and given serum-free media for 6 hours. Proteins were harvested as described below. Tumor tissue was first homogenized using TissueMiser (Fisher Scientific) and directly lysed in RIPA Buffer containing a c0mplete Mini, EDTA-free protease inhibitor cocktail (Roche) and phosphatase inhibitor cocktail (Sigma, followed by centrifugation (4°C, 10 000xg, 15 min). Protein was quantified using a DC™ Protein Assay (Bio-Rad Laboratories), separated and transferred to PVDF membranes using standard western blot conditions. Antibodies used are listed in Supplemental Table 1. Membranes were washed with TBST. Primary and secondary antibodies were diluted in 5% BSA. Immunolabeled proteins were visualized using ECL Western Blot Detection Reagent (Amersham).

AGDEX Analysis

Differential gene expression was calculated as the difference between the means of normal tissues and tumor samples for 10,698 genes orthologous between human and mouse. This difference was calculated in human (*d1*) and mouse (*d2*) samples separately, and results represented as a vector in multi-dimensional space. The AGDEX statistic is the cosine of the angle between *d1* and *d2* in multivariate space.

Differentiation quantification algorithm

Image analysis algorithm consists of two steps: 1) finding the optimal intensity threshold to segment myotubes; 2) nuclei segmentation and calculation of the fusion index. For the first step all the MyHC-channel images were thresholded based on Otsu's method (Otsu, 1979), using a custom MATLAB (MathWorks) script. 25th percentile across all the measured thresholds was used as a global threshold to generate myotube masks. As the next step, images were processed using a custom Columbus (PerkinElmer) script to segment nuclei and measure area of the myotubes as well as nuclei within the myotubular mask. MATLAB and Columbus scripts are available upon request.

REFERENCES

Otsu, N. (1979). A Threshold Selection Method from Gray-Level Histograms. Systems, Man and Cybernetics, IEEE Transactions on *9*, 62-66.

SUPPLEMENTARY TABLE LEGENDS

Supplementary Table 1. Source and use of reagents, including antibodies, primers and drugs.

Supplementary Table 2. AC50 and Percent Area Under the Curve (% AUC) values for 1912 drugs screened in the M25.FV24c tumor-derived cell line.

SUPPLEMENTAL TABLE

Supplemental Table 1

Primary Antibodies:			
Antigen (acronym) [clone]	**Source**	**Host**	**Dilution (Usage[a])**
Desmin [D33]	Dako	Mouse	1:50 (IHC)
Fibroblast growth factor receptor 4 (FGFR4) [C16]	Santa Cruz Biotechnologies	Rabbit	1:1000 (IB)
Keratin [AE3]	Millipore	Rabbit	1:50 (IHC)
MyoD1 [5.8A]	Dako	Rabbit	1:100 (IHC)
Myogenin [F5D]	Becton Dickinson	Rabbit	1:100 (IHC)
Myosin Heavy Chain (MyHC) [MF20]	R&D Systems	Mouse	1:200 (ICC) 1:1000 (IB)
S100A4	Dako	Rabbit	1:200 (IHC)
Smooth muscle actin (SMA) [1A4]	Dako	Mouse	1:200 (IHC)
α-tubulin [DM1A]	Sigma	Mouse	1:5000 (IB)
CyTOF Antibodies:			
Cleaved Caspase3-142Nd [C92-605]	BD Biosciences	Mouse	1:200 (CyTOF)
phospho-4EBP1-149Sm (Tyr37/46) [M31-16]	BD Biosciences	Mouse	1:200 (CyTOF)
phospho-AKT-152Sm (Ser473) [M89-61]	BD Biosciences	Mouse	1:200 (CyTOF)
phospho-p38 MAPK-156Gd (pT180/pY182) [36]	BD Biosciences	Mouse	1:300 (CyTOF)
phospho-p44/42 MAPK (ERK1/2)-167Er (Thr202/204) [20a]	BD Biosciences	Mouse	1:300 (CyTOF)
phospho-S6-175Lu (Ser235/236) [N7-548]	BD Biosciences	Mouse	1:400 (CyTOF)
phospho-SRC-159Tb (Tyr418) [K98-37]	BD Biosciences	Mouse	1:50 (CyTOF)
phospho-STAT1-153Eu (pY701) [4a]	BD Biosciences	Mouse	1:300 (CyTOF)
phospho-STAT3-158Gd (Y705) [4/P-STAT3]	BD Biosciences	Mouse	1:200 (CyTOF)
phospho-STAT5-151Eu (Tyr694) [47]	BD Biosciences	Mouse	1:400 (CyTOF)
Isotype Control Antibodies:			
Mouse IgG	Santa Cruz Biotechnologies	Mouse	[b] (ICC)
Rabbit IgG	Santa Cruz Biotechnologies	Mouse	[b] (ICC)
Secondary Antibodies:			
Anti-mouse IgG-AlexaFluor488	Molecular Probes	Donkey	1:500 (ICC)
Anti-mouse IgG-HRP	GE Healthcare	Sheep	1:5000 (IB)
Anti-rabbit IgG-HRP	Santa Cruz Biotechnologies	Goat	1:5000 (IB)
Real-Time PCR Primers:			
Gene Symbol (Accession Number)	**Primer Sequence (5′→3′)**	**T_a (°C)[c]**	**Amplicon (bp)**
Myod1 (NM_010866)	F:CCCGGCGGCAGAATGGCTAC R:GGAGTGCCTACGGTGGTGCG	60.0	86
Myog (NM_031189)	F:GCAATGCACTGGAGTTCG R:ACGATGGACGTAAGGGAGTG	60.0	94

Myf5 (NM_008656)	F:ACAGCAGCTTGACAGCATC R:AAGCAATCCAAGCTGGACAC	60.0	85
Myf6 (NM_008657)	F:GCCTCGTGATAACTGCTAAGG R:GTTCCAAATGCTGGCTGAGT	60.0	162
Gapdh (NM_001289726)	F:GGTGCTGAGTATGTCGTGGA R:ACAGTCTTCTGGGTGGCAGT	60.0	290
Actb (NM_007393.3)	F:GGCTGTATTCCCCTCCATCG R:CCAGTTGGTAACAATGCCATGT	60.0	154
Proviral Integration PCR Primers:	**Primer Sequence**	**T_a (°C)[c]**	**Source**
PGK-forw	TCGACCCACTATGGGAGTTC	60.5	Addgene
FGFR4-R6	GGAGGTCGAGGTACTCCTCA	62.5	In house
FGFR4 Sequencing PCR Primers:			
PGK-forw	TCGACCCACTATGGGAGTTC	60.5	Addgene
FGFR4-R6	GGAGGTCGAGGTACTCCTCA	62.5	In house
FGFR4mut-F	GCCAGGTAGTACGTGCAGAGGC	67.9	In house
FGFR4mut-R	AACTCCCGCAGGTTTCCCTTG	63.2	In house
p53 Genotyping PCR Primers			
p53x6.5	F:ACAGCGTGGTGGTACCTTAT	60.0	Jackson Laboratory[e]
p53x7	R:TATACTCAGAGCCGGCCT	60.0	Jackson Laboratory[e]
p53xNeo	F:CTATCAGGACATAGCGTTGG	60.0	Jackson Laboratory[e]
Drugs			
Compound	**Source**	**Stock**	**Vehicle**
Vincristine Sulfate	Toronto Research Chemicals	1 mM	Methanol
GSK2126458	ChemieTek	10 mM	DMSO

[a]: Abbreviations: ICC: immunocytochemistry, IHC: immunohistochemistry, IB: immunoblot
[b]: Dilution dependent on concentration of protein-specific primary antibodies
[c]: Primer annealing temperature
[d]: Primer bank (pga.mgh.harvard.edu/primerbank/)
[e]:jaxmice.jax.org/protocolsdb/f?p=116:2:3868241449886939::NO:2:P2_MASTER_PROTOCOL_ID,P2_JRS_CODE:5741,002101

SUPPLEMENTAL FIGURES

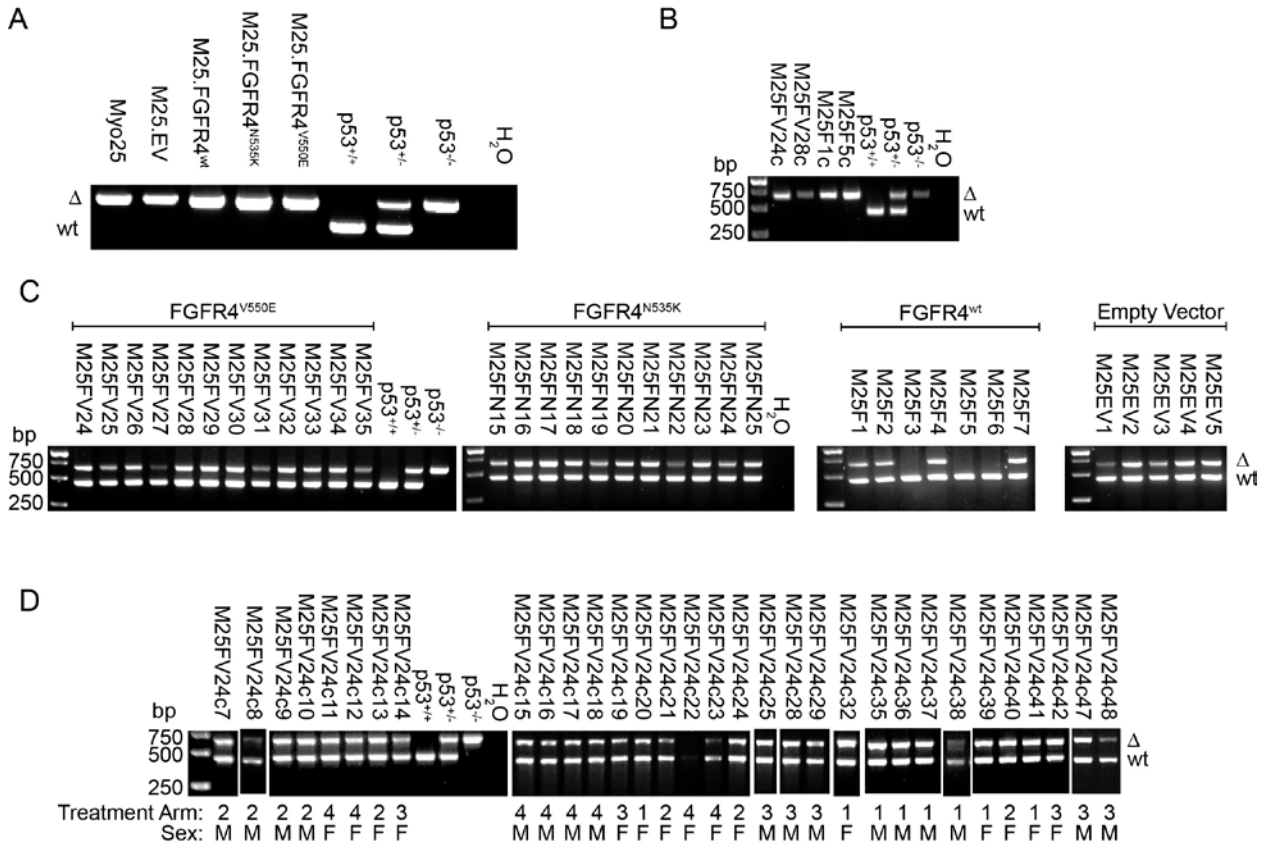

Supplemental Figure 1. p53 genotype in primary cell lines and experimental mice confirmed using standardized PCR. (A) Myoblast and tumor-derived (B) cell lines were all shown to encode only the p53 mutant allele (Δ) when compared to mice with known genotypes (wildtype $p53^{+/+}$, heterozygous $p53^{+/-}$ and null $p53^{-/-}$). Reactions performed with no DNA template (H_2O) were used as negative controls. (C) All experimental mice were genotyped from primary and secondary tumor models, including GSK2126458 study (D).

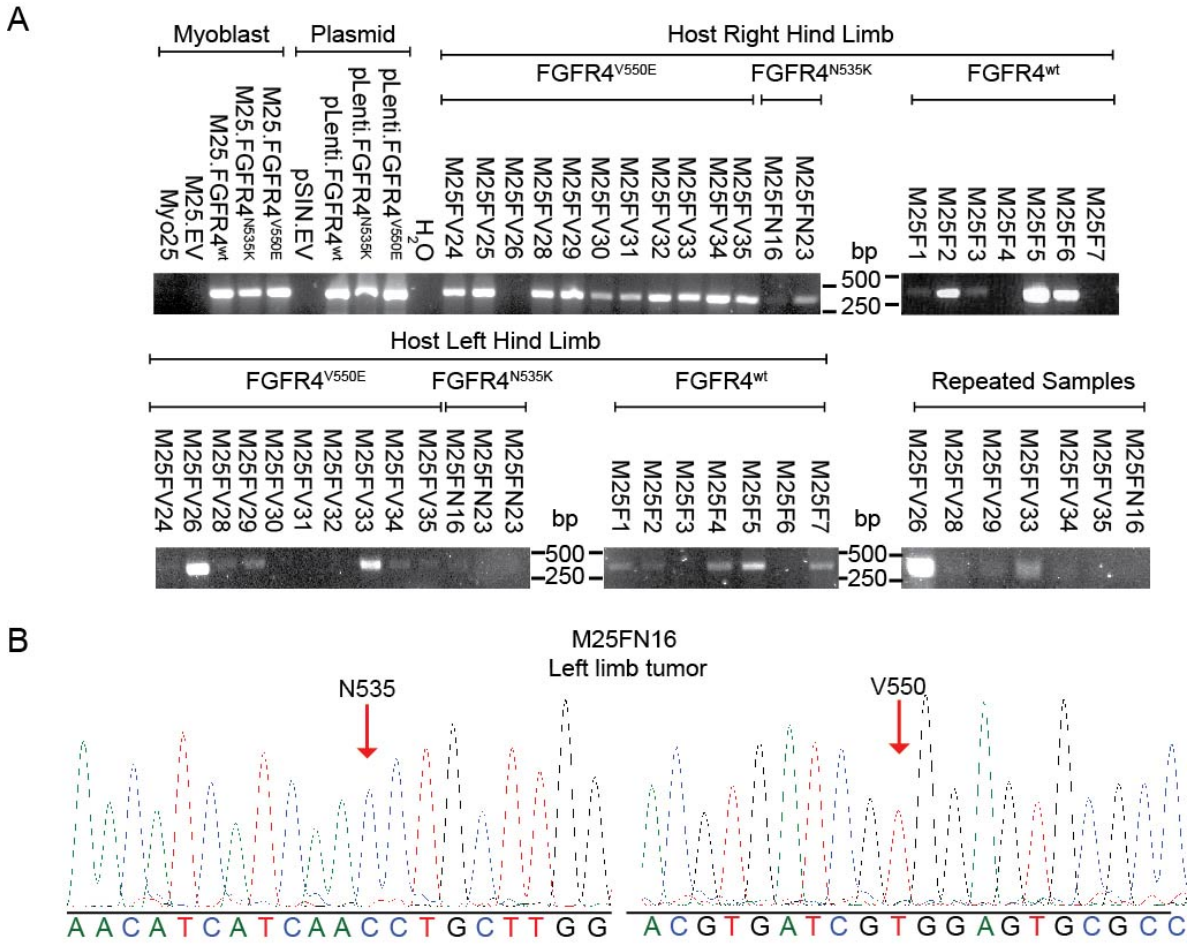

Supplemental Figure 2. Proviral integration was confirmed in myoblasts and tumors with PCR. (A) Parental, empty vector control, and FGFR4 over-expressing myoblasts and tumors were subjected to PCR using transgene-specific primers (Figure 1A) and visualized on ethidium bromide stained agarose gels following electrophoresis. Plasmid DNA was used as positive and negative controls. Tumor samples were interrogated using this technique. (B) Sequencing of PCR amplicons from the left hind limb tumor in the M25.FGFR4^{N535K}-injected cohort (M25FN16) confirmed that this tumor encoded FGFR4^{wt}.

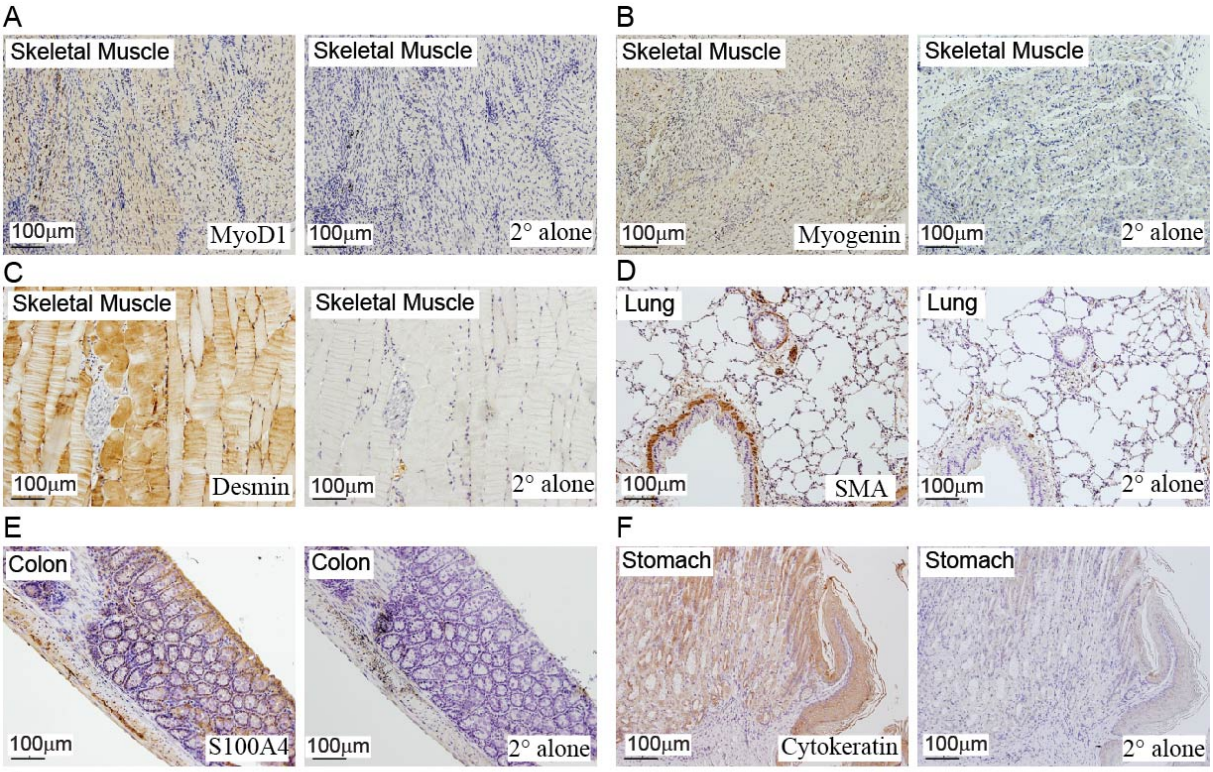

G

Injected Cells	Sample	MyoD1	Myogenin	Desmin	SMA	S100A4	Cytokeratin	Diagnosis
M25.FGFR4^{wt}	M25.F1	0	0	0	0	0	0	High-grade sarcoma, undifferentiated
M25.FGFR4^{wt}	M25.F2	0	0	0	0	0	0	High-grade sarcoma, undifferentiated
M25.FGFR4^{wt}	M25.F3	2	0	3	0	0	0	High-grade sarcoma, rhabdomyoblastic differentiation
M25.FGFR4^{wt}	M25.F5	0	0	0	0	0	0	High-grade sarcoma, undifferentiated
M25.FGFR4^{wt}	M25.F6	0	0	0	4	0	0	High-grade sarcoma, myoid differentiation
M25.FGFR4^{wt}	M25.FN16	0	0	2	3	0	0	High-grade sarcoma, myoid differentiation
M25.FGFR4^{N535K}	M25.FN23	0	0	0	5	0	0	High-grade sarcoma, myoid differentiation
M25.FGFR4 ^{V550E}	M25.FV24	0	0	0	1	0	0	High-grade sarcoma, myoid differentiation
M25.FGFR4 ^{V550E}	M25.FV25	0	0	0	1	0	0	High-grade sarcoma, myoid differentiation
M25.FGFR4 ^{V550E}	M25.FV26	0	0	0	4	0	0	High-grade sarcoma, myoid differentiation
M25.FGFR4 ^{V550E}	M25.FV28	0	2	4	N/A	0	0	High-grade sarcoma, rhabdomyoblastic differentiation
M25.FGFR4 ^{V550E}	M25.FV29	1	1	2	0	0	0	High-grade sarcoma, rhabdomyoblastic differentiation
M25.FGFR4 ^{V550E}	M25.FV30	0	0	0	5	0	0	High-grade sarcoma, myoid differentiation
M25.FGFR4 ^{V550E}	M25.FV31	0	0	0	4	0	N/A	High-grade sarcoma, myoid differentiation
M25.FGFR4 ^{V550E}	M25.FV32	4	2	4	N/A	0	0	High-grade sarcoma, rhabdomyoblastic differentiation
M25.FGFR4 ^{V550E}	M25.FV33	1	2	2	N/A	0	0	High-grade sarcoma, rhabdomyoblastic differentiation
M25.FGFR4 ^{V550E}	M25.FV34	1	2	1	N/A	0	0	High-grade sarcoma, rhabdomyoblastic differentiation
M25.FGFR4 ^{V550E}	M25.FV35	0	0	0	4	0	0	High-grade sarcoma, myoid differentiation

Score	% positive
0	none
1	<1%
2	1-10%
3	10-33%
4	22-66%
5	>66%
N/A	Not assessed

Supplemental Figure 3. Control stains for murine tumor histopathological analysis. Tumors were subjected to detailed histopathological review using a panel of lineage-specific antibodies. All tumors were negative for S100 and pan-cytokeratin, thereby excluding neural crest and epithelial derivations, respectively. Only tumor cells were examined for immunopositivity and confounding entrapped native, particularly atrophic and regenerating skeletal muscle was avoided. Juvenile skeletal muscle was used as positive control for expression of skeletal muscle markers, MyoD1 (A), Myogenin (B) and Desmin (C). Lung tissue was used as a positive control for the smooth muscle marker, SMA (D). Colonic tissue (neural plexus) was used as positive control for S100A4 (E). Gastric mucosa was used as positive for the epithelial marker Cytokeratin (F). Negative controls show tissue stained with secondary antibodies only.

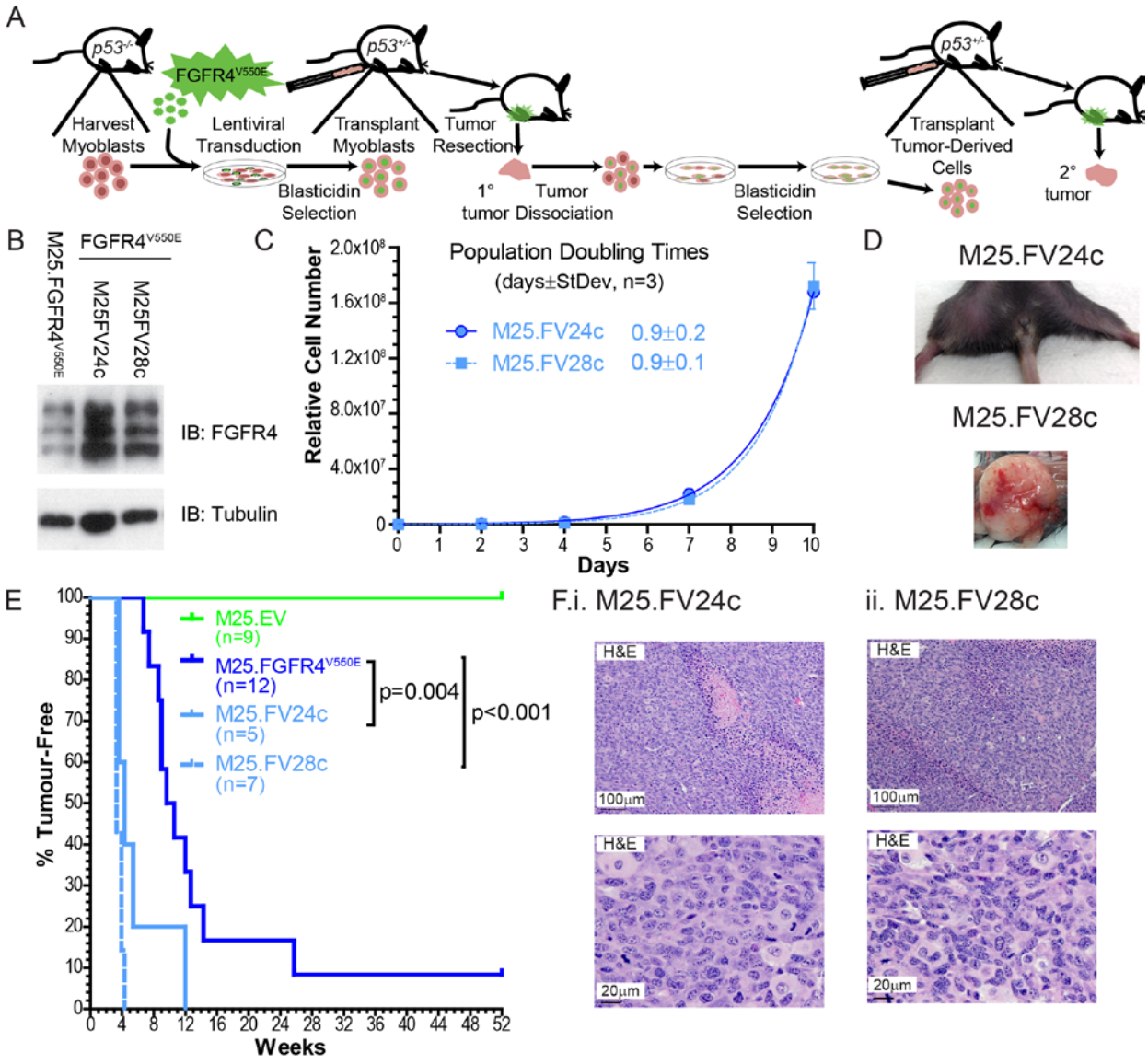

G

Injected Cells		Host Mice	Tumors		
Right Limb	Left Limb	Genotype	Penetrance (n)	Mean Latency (weeks) (Range)	Median Latency (weeks)
M25.FV24c	-	p53+/-	100% (5/5)	4.0 (4-5 weeks)	4.2
M25.FV28c	-	p53+/-	100% (7/7)	3.3 (3-4 weeks)	3.6

Supplemental Figure 4. Secondary tumor models were generated using cell lines derived from M25.FGFR4^{V550E} tumors. (A) Schema depicting the generation of secondary tumors using cells harvested from M25.FGFR4^{V550E} tumors that were selected using Blasticidin and engrafted into syngeneic host hind limbs. (B) Tumor-derived cell lines, M25.FV24c and M25.FV28c, immunoblotted using human FGFR4-specific antibodies, demonstrating human FGFR4 overexpression in FGFR4^{V550E} tumor-derived cell lines. (C) Population doublings of M25.FV24c and M25.FV28c were calculated from 3 independent 10-day proliferation assays (representative curves shown) revealing doubling times of 1 day for both cell lines. (D) Tumors formed in the right hind limbs of mice following injection of M25.FV24c and M25.FV28c. (E) Survival curves compare tumor-free survival of M25.FV24c and M25.FV28c compared to the M25.FGFR4^{V550E}-injected cohort from which the cell lines were generated and the M25.EV control cohort. (F) H&E staining of M25.FV24c (i.) and M25.FV28c (ii.) demonstrated consistent morphology with primary tumors. (G) Table depicting penetrance and latencies of secondary tumors formed following injection of tumor-derived cells, M25.FV24c and M25.FV28c.

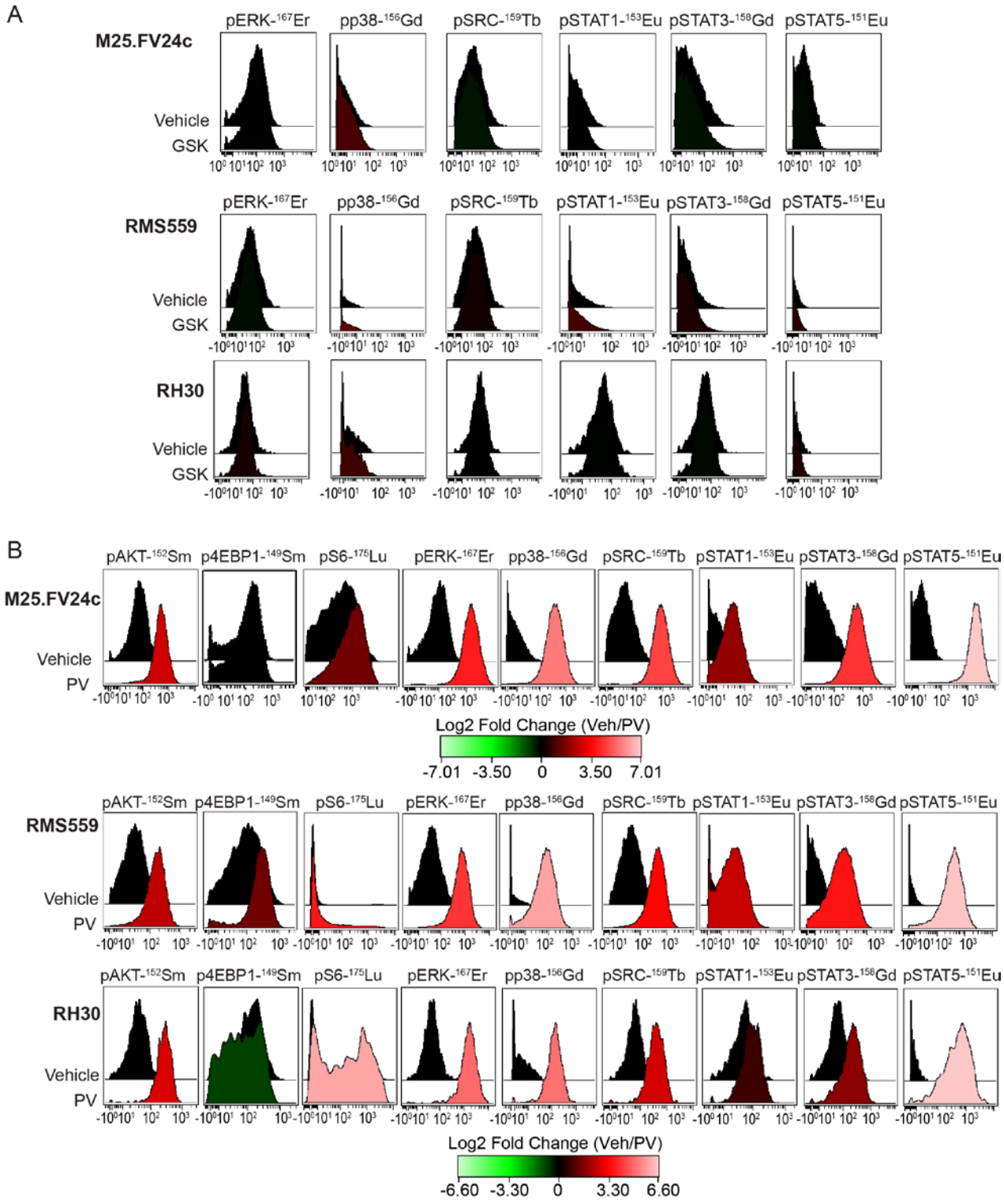
A
pERK-167Er
pp38-156Gd
pSRC-159Tb
pSTAT1-153Eu
pSTAT3-158Gd
pSTAT5-151Eu
M25.FV24c
Vehicle
GSK
RMS559
RH30
B
pAKT-152Sm
p4EBP1-149Sm
pS6-175Lu
M25.FV24c
Vehicle
PV
Log2 Fold Change (Veh/PV)
-7.01 -3.50 0 3.50 7.01
RMS559
RH30
-6.60 -3.30 0 3.30 6.60

Supplemental Figure 5. Mass cytometric analysis of murine and human RMS cell lines demonstrates selective inhibition of mTOR signalling. (A) Histogram overlays depicting M25.FV24c and human cell lines RMS559 and RH30 treated for 30 min with 40 nM GSK2126458 (GSK) or vehicle. These plots demonstrate that phosphorylation of ERK, p38 MAPK, SRC, pSTAT1, pSTAT3 and pSTAT5 was very low to moderate in murine or human RMS cells but was not decreased by GSK2126458 treatment suggesting that the PI3K/mTOR signaling does not regulate activity of the RAS/MAP, SRC and JAK signaling pathways in RMS cells. Log_2 fold change ratio scales are the same as below. (B) Mass cytometry histogram overlays depicting M25.FV24c, RMS559 or RH30 cells treated for 20 min with either vehicle or the phosphatase inhibitor pervanadate (PV). These plots demonstrate that AKT, mTOR, RAS/MAP, SRC and JAK signalling pathways can be activated in murine and human RMS cell lines. Histograms were coloured using the indicated scale to reflect the Log_2 FC ratio of the median metal intensity of each marker.

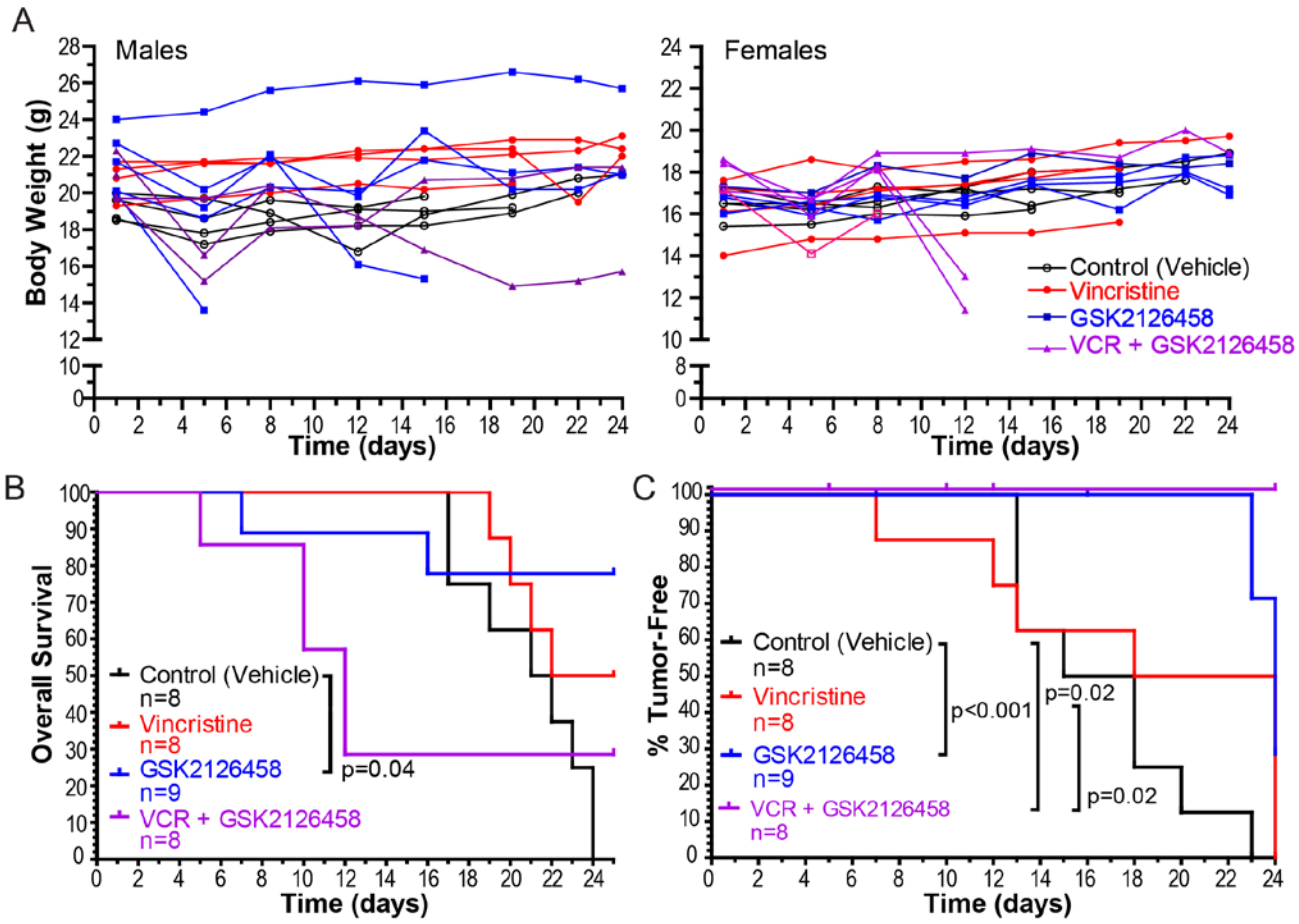

Supplemental Figure 6. Additional data from experimental mice treated in the GSK2126458 study. (A) Graphs illustrating mouse body weight for male and female test subjects over the course of the experiment. (B) Kaplan-Meier curves demonstrating overall survival and tumor-free survival (C) of mice in the 4 treatment arms.